Application of Polypyrrole Actuators: Feasibility of Variable Camber Foils

John D. W. Madden, Bryan Schmid, Martin Hechinger, Serge R. Lafontaine, Peter G. A. Madden, Franz S. Hover, Richard Kimball and Ian W. Hunter

***Abstract*— A decade of research into electroactive polymer actuators is leading to the exploration of applications. These technologies are not ready to compete with the internal combustion engine and electric motors in high power propulsion systems but are suitable for intermittent or aperiodic applications with moderate cycle life requirements, providing an alternative to solenoids and direct drive electric motors. Polypyrrole, an emerging actuator material, is applied to drive hydrodynamic control surfaces and in particular to change the camber of a foil. The foil is intended for use in the propeller blade of an autonomous underwater vehicle. A scaled prototype is constructed which employs polypyrrole actuators imbedded within the blade itself to vary camber. The kinematics required to generate camber change are demonstrated, with > 30^o deflections of the trailing edge being observed from both bending bilayer and linear actuator designs. Forces developed in still conditions are five times lower than the 3.5 N estimated to be required to implement variable camber. The observed 70 kJ/m^3 polypyrrole work density however is more than sufficient to produce the desired actuation from within the limited blade volume, enabling an application that is not feasible using direct drive electric motors. A key challenge with the polypyrrole actuators is to increase force without sacrificing speed of actuation.**

***Index Terms*—Actuator, Autonomous Underwater Vehicle, hydrodynamics, Artificial Muscle, Conducting Polymer, Control Surface, Electroactive, EAP.**

I. Introduction

Electroactive polymer (EAP) research has reached a level of maturity such that applications are actively being sought and developed, as evidenced by the number of application related papers presented at the annual conference on EAPs [1]. Where new technologies are being introduced, it seems appropriate to seek applications in which distinct advantages over existing technology are offered. In this paper the feasibility of using conducting polymer actuators to vary the camber of propeller blades in autonomous underwater vehicles is investigated. Although the application is very specific, the experiments and analysis performed here will provide guidance in the general design issues and concerns encountered in applying EAPs. In combination with other papers in this issue – including a general review of artificial muscle technologies by [2], and a specific look at operating conditions and limitations in polypyrrole actuators [3] – a comprehensive perspective on the application of artificial muscle technologies, and in particular conducting polymer actuators, is offered.

A. Application of artificial muscle technologies: Where are the Opportunities?

Established actuator technologies [4] for which artificial muscle technologies might offer an alternative include internal combustion engines, high-revving electric motors, direct drive electric motors, and piezoelectric actuators.

1) Propulsion Systems and Artificial Muscle

Competing with the internal combustion engine for propulsion of surface vehicles such as automobiles and ships is a challenge due to the high power to mass of these motors (1000 W/kg) [4] and the high energy density fuel (43 MJ/kg) employed. Fuel cells and hybrid engines can provide high energy density electrical energy sources, making the use of high revving electric motors feasible. Electric motors offer power densities similar to the internal combustion engine and efficiencies that can exceed 90 % [4]. Only shape memory alloys and piezoceramic actuators can clearly surpass the power to mass of internal combustion engines and electric motors [5]. Piezoelectrics however generate very small strains (~0.1 %) and thus it is a great challenge to use them to generate large displacements. Shape memory alloys however are too low in electromechanical efficiency and cycle life to consider for continuous large scale propulsion [2,5].

Underwater the energy equation changes substantially, as combustion engines and fuel cells rely on oxygen, which must be transported (unless dissolved oxygen or air bubbles are collected). Combustion of hydrocarbons is not particularly advantageous over battery power [6] undersea since battery driven electric motors are more practical for use in propulsion of submersibles.

New actuator materials such as dielectric elastomers, ferroelectric polymers, conducting polymers and carbon nanotubes can offer power to mass ratios that are within a factor of 4 of the combustion engine [2]. The lower power densities of these materials may be compensated for by their 'muscle-like' nature, making them more suitable for

Manuscript received October 23, 2003. This work was supported in part by the Office of Naval Research STTR program.

J. Madden is with the University of British Columbia, Vancouver, Canada, V6T 1Z4 (email: jmadden@ ece.ubc.ca) and Molecular Mechanisms LLC, Lincoln, MA, USA. M. Hechinger is also with the University of British Columbia.

B. Schmid and S. Lafontaine were working for Molecular Mechanisms LLC and are now with the BioInstrumentation Laboratory at MIT in Cambridge Massachusetts, USA, which is led by I. Hunter.

P. Madden is with the Department of Organismic and Evolutionary Biology at Harvard University, Cambridge MA, USA.

F. Hover & R. Kimball are with the Department of Ocean Engineering at MIT.

biomimetic propulsion [7,8]. However, there are a number of challenges for system designers [9]. For example, dielectric elastomers and ferroelectric polymers operate at kilovolt level voltages, requiring DC-DC voltage conversion where battery power is employed. Lower voltage actuators based on conducting polymers, carbon nanotubes, and ionically conductive polymer metal composites currently suffer from poor electromechanical coupling [2]. Finally, none of the emerging actuator technologies have demonstrated cycle lifetimes of more than 10^7 [2] (in some cases the cycle life has yet to be properly measured). Continuous operation at 10 Hz may lead to failure after 10 days or less. Although the new actuator technologies are expected to improve in many respects [2], at present they do not offer compelling alternatives to electric motors and combustion engines for high power, continuous propulsion.

2) Intermittent Actuation

Vehicular propulsion typically involves continuous rotation of wheels or screws, activities for which internal combustion engines and high revving electric motors are well suited. Discontinuous and aperiodic motions such as the grasping of parts by a robot arm, the opening of a valve or the adjustment of a hydrodynamic control surface are not easily performed using rapidly spinning actuators with relatively narrow ranges of optimal rotation rates. In such cases direct drive electric motors are often employed. However the low force, torque and work to mass ratios of these direct drive actuators means that they are relatively heavy and bulky [4]. For example, Honda's sophisticated humanoid Asimo robot, which relies on servo-motors for movement, does not have much torque to spare after lifting its own weight, thereby limiting the impact its legs can sustain, and in turn preventing walking speeds from exceeding 2 km/hr [10]. A further disadvantage of the electromagnetic actuators is that they expend energy to hold a force, even when no mechanical work is being performed. Holding a fixed position under load is thus highly inefficient, unless a catch or lock can be implemented. Applications of a discontinuous nature occurring in situations where the space and or mass are at a premium, as in autonomous underwater vehicles (AUVs), could benefit from actuators with higher force and work densities that feature catch states. One such application which will be examined further is the positioning of hydrodynamic surfaces in order to change camber.

3) Anticipated Advantages of Variable Camber Propellers

Deflection of key areas of a propeller blade (such as the leading and trailing edges) leads to large changes in loading resulting from only small input forces [11]. Such a variable camber blade geometry is expected to offer many of the advantages of the controllable pitch propeller [12], which include:

- Better off-design efficiency: efficient multimode operation;
- Ability to adjust load to match engine or motor characteristic;
- Cavitation mitigation under heavily loaded conditions (acceleration, towing etc.);
- Ability to produce rudder flow at low vessel speeds to help low speed maneuvering;
- Ability to operate in reverse thrust condition without changing shaft rotation direction;
- Elimination of gearbox (though a reduction gear may still be required).

Distinct advantages of variable camber are:

- Elimination of gearboxes;
- Electronic actuation of the propeller blade geometry;
- No gears/shafting is required for the actuators;
- There is potential for individual blade control with minimal increase in system complexity;
- A simplified control driver is easily controlled by a computer.

These anticipated advantages are made possible by the voltage control, and by the relatively high energy densities and forces produced by artificial muscle materials [2], enabling these actuators to be incorporated into blades, and eliminating the need for transmission down the shaft.

The mechanical complexity and cost of pitch control mechanisms is the major disadvantage of such propellers. The mechanism requires gearing in the hub for each blade as well as control rods embedded in the propeller shaft and actuators inside the ship, thus requiring more complex sealing than a simple shaft [12]. Such systems are relatively expensive in comparison to fixed pitch propellers, and require more maintenance to ensure reliability [12]. For these reasons controlled pitch propellers have been primarily limited to large vessels where economies of scale are most attractive.

An inexpensive mechanism that replaces variable pitch propeller mechanisms is potentially of great value in small vessels.

4) Illustration of the efficiency gained by using variable camber propellers.

The following example illustrates the effect of load on the efficiency of a typical fixed propeller powered by a DC electric motor. Figure 1a shows the motor performance curve of a typical DC motor along with the torque speed characteristics of a fixed propeller operating on a hull with quadratic resistance vs. speed (i.e., a streamlined underwater hull). Under these conditions the propeller efficiency is roughly constant and if well designed will be near its maximum efficiency under typical operating conditions. However, as the speed of the vessel is changed the operating point moves off the motor's efficiency peak. By incorporating a variable geometry propeller, the operating point can be moved to better match the motor's performance as shown in Figure 1b. Such matching is not achievable with a fixed propeller system. The increase in efficiency is potentially very valuable in AUV's and related vehicles where energy and space are very restricted.

Efforts are underway to experimentally quantify the benefits of variable camber propulsion. The aim of this paper is to show the feasibility of employing new actuator materials [2], and in particular polypyrrole, to achieve variable camber, and to elucidate the advantages and challenges in employing this actuator technology in discontinuous and quasi-steady applications. In particular the following questions are addressed: Is polypyrrole an appropriate actuator technology for such applications?; What are polypyrrole's advantages and disadvantages compared to alternatives?; How significant are the challenges in scaling up this technology from the laboratory scale (milliJoule energy scale, millimeter displacements) to the device scale?; What are the prospects for application in AUVs and other systems?

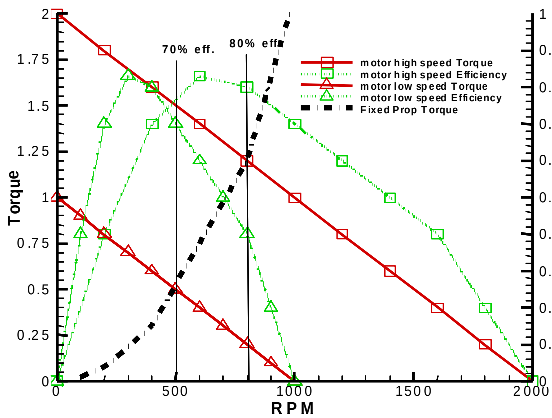

Fig 1a: Operating curves of a motor/prop/hull with a fixed propeller.

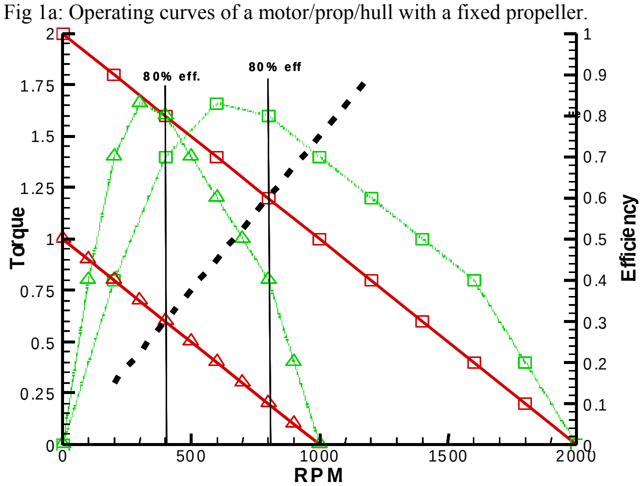

Fig 1b**:** Capabilities of a variable-geometry propeller with the same motor & hull as in Figure 1a. The propeller torque/speed relationship (dashed line) is shown to be modified in order to optimize efficiency.

Before reporting on the experimental feasibility of employing polypyrrole actuators in variable camber systems, the desired performance is established, and the selection of polypyrrole is justified. After setting the specifications, two prototypes are described which were built with dimensions appropriate for ultimate testing in the MIT water tunnel, and are thus larger in volume than required in the final vehicle. Scaling is used to estimate the feasibility of their use on the desired scale. The kinematics, force generation and water tightness are tested. It is shown that the devices meet the kinematic requirements. Forces need to be increased in order to achieve the performance targets. Time required to develop peak force is approximately 50 s in one device and tens of minutes in the other, and thus means of increasing speed will be required.

II. Specifications

The target vehicle for variable camber is the Expendable, Mobile Anti-submarine warfare Training Target (EMATT) from Sippecan Inc, in Marion, Massachusetts [15]. The vehicle is designed to act as a target for antisubmarine warfare exercises, and as such is expendable.

Minimum actuator/propulsor performance specifications are determined based on the EMATT speed and geometry.

Force: The streamlined EMATT vehicle is 100 mm in diameter and 900 mm length, and is geometrically similar to a Remus vehicle, whose specifications have been reported [13]. Remus requires 6.8 N of thrust to operate at 1.5 m/s (3 knots); it has a 165 mm diameter and fineness ratio (L/D) varying from six to eleven. For a general idea of what forces are required in the EMATT vehicle, scaling is performed with the ratio of speeds squared, and the ratio of diameters squared. Operating at 1.5 m/s EMATT generates approximately 2.9 N of drag force. At the upper speed limit of 4 m/s, 21 N of drag force is expected. With three blades per propeller, the upper load limit is 7 N per blade acting over a span of about 50 mm (accounting for duct thickness and a small hub). Actuated trailing edges used for variable camber control will sustain less than half of the 7 N since the majority of the load is carried by the main solid core of the blade [11]. Thus less than 3.5 N per blade is born by the trailing edge and must be withstood by the actuator.

Implications of Force Estimates: Trailing Edge Designs

Based on Riegels' data [11] of blade pressures, as the flap is altered from its nominal position to ± 22 degrees there is a large change in foil lift. The force on the trailing edge to achieve this lift change is small in comparison with the relative overall lift change [11] and therefore the controllable surface in this area of the foil will require only a relatively small actuation force to achieve a large change in overall lift. Riegels shows that pressures are very large near the leading edge of the foil – as a result, leading edge actuation requires

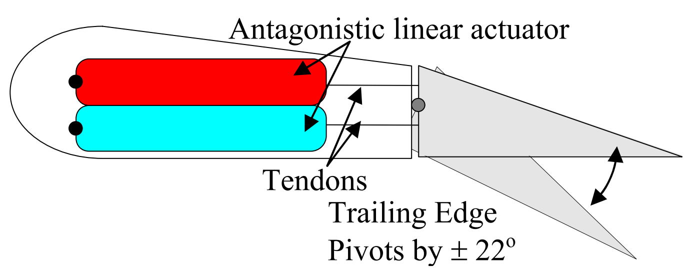

Figure 2: Lever arm design for creating variable camber. The triangular tail section pivots about a joint (gray circle). Torque is applied to the trailing edge section via an antagonistic actuator pair coupled via tendons.

substantially larger forces than at the trailing edge. Hence, in this work, camber is varied using the trailing edge only.

Displacement/Camber change: The extent of displacement of the trailing edge has yet to be optimized. A trailing edge deflection of up to ±22 degrees occurring on the last 25-40 percent of the chord is chosen to emulate common high-lift flap geometries [14].

Mission Life: EMATT is a single use vehicle. The device must operate over a time period of 24 hours without failure (the maximum mission duration). Assuming that camber variations are needed at most once every minute on average, the upper bound on number of cycles sustained by the moveable flap is 1500.

Environment: The EMATT performs shallow dives, attaining relative pressures of up to ~ 2 MPa. The vehicle must also be able to withstand a corrosive aqueous environment.

Cost: The cost limit remains to be determined, but current low-cost thruster assemblies of motors, shafting, and propellers are in the range of $100-400 per vehicle [15]. Our objective is to minimize the additional cost resulting from the added degrees of freedom.

Aft Volume: The EMATT vehicle has a fairly large open area in the after-body as the motor is situated well forward. The motor shaft is connected to the through-hull shaft with a flexible coupling. Suitably mounted, several electronic packages of > 15 cm^3 each can easily be entrained, providing control and power to the propeller.

Power Connection: Fifteen DD size primary Lithium-Sulfur dioxide batteries with nominal voltages of 3 V provide a total energy total of 3 MJ [15].

Actuator Requirements: The next step is to calculate the forces, displacements, work densities, rates and cycle life required of the actuators. Each EMATT propeller blade has an approximate span (length) of 50 mm, a chord (width) of 25 mm, and an average thickness of 6 mm. In our design the last 10 mm of the chord at the trailing edge will be pivoted so as to enable variable camber. Figure 2 shows the approximate geometry. The angle of the trailing edge is to be adjusted by ±22 ° under a load of up to 3.5 N.

The unknown distribution of blade loading force is assumed to be applied at a single point 3 mm from the trailing edge, or, equivalently, 7 mm from the pivot point. The force of 1.75 N generates a torque of T=25 mN·m about the pivot. If the total deflection is θ=44°, the maximum work that must be done is $W = T\cdot\theta = (25\ \text{mN m})\times(\pi/4) = 19$ mJ.

A key objective is to avoid the need for mechanical transmission down the shaft to reach the propeller. Ideally the mechanism employed will fit within a propeller blade. The non-pivoting portion of each blade has a volume of 6 mm × 15 mm × 50 mm = 4.5×10^{-6} m^3. Given the required work, the minimum work density in order to fit the actuator within the propeller volume is ~ 4.2 kJ·m^{-3}. In fact the work density will need to be at least double this value, or > 8 kJ·m^{-3} as otherwise no space is allotted for structural elements, power delivery, encapsulation, electrodes, electrolyte and sensors.

Assuming adjustment of the camber takes place over 1 to 10 s, the output power is 1.9 to 19 mW.

III. Actuator Selection & Challenges

The results presented here do not represent the first time artificial muscle technologies have been applied to fluid dynamic problems. Bandyopadhyay et. al. employed ionically conductive polymer metal composites to show that oscillating the trailing edge 'flap' of variable camber blades in a propeller appears to increase thrust, and thus should enable lower RPM operation of propellers, and reduced noise emission [16]. Reynaerts [17] and Beauchamp [18] have demonstrated the use of shape memory alloys to vary camber in wings and control surfaces in general. Given this history, why choose polypyrrole actuators over other emerging and established technologies? In this section the rationale for choosing polypyrrole actuators is presented [9].

The number of actuator technologies capable of meeting the work density and other requirements in order to fit within the propeller blade is limited. Candidate actuator technologies are now discussed.

DC Servo Motors: Direct drive electric motors are a well established, commercially available technology. These are powered by DC voltages readily obtained from a submersible's battery. There is a strong incentive to employ such established technology where possible. However these do not exhibit sufficient torque given the available volume for direct drive application [19]. Custom motors optimized for torque production have attained torque to mass ratios of 10 N·m/kg [20], about 5 times greater than are observed in conventional motors [19]. However, as with the other direct drive electric motors a catch mechanism or servo control is needed to maintain position. The parallel disk geometry is even worse than the tetragonal shape of most motors for making effective use of the hydrofoil volume, they are not commercially available, and are challenging to build due to their magnetically unstable configuration [20]. For these reasons alternative actuator technologies are considered.

Emerging actuator materials: Recently a number of new actuating materials have emerged that generate sufficient force and energy to make them promising candidates for enabling in situ propeller shape changes [2]. Of these, dielectric elastomers, ferroelectric polymers, and conducting polymers have sufficient work density to fit within the blade dimensions, and appear to offer the necessary degree of position control [2,9]. Furthermore, unlike electric motors they can work against a constant force without requiring energy input. Finally, the magnitude of the applied potential and the extent of charge transfer can be used to predictably set the stress-strain state of these actuators. Thus these materials are readily controllable (unlike shape memory alloys [2]).

Dielectric elastomers are rubbery materials (silicones and acrylics) which, when used as the dielectric in a capacitor, deform when fields are applied due to the attraction between capacitor electrodes [2,9]. Relaxor ferroelectric polymers feature polar groups on the polymer backbone which are realigned by applied fields, leading to dimensional changes [2]. Dielectric elastomers and ferroelectric polymers typically require activation potentials on the order of several kilovolts.

Conducting polymer actuators are composed of conjugated polymers that are electronically conductive. Dimensional changes are observed in response to changes to electrochemically induced changes oxidation state [2]. Applied potentials are in the range of 1 V to 10 V.

Each of these emerging actuator technologies has significant advantages and challenges associated with it. Both dielectric elastomers and ferroelectric polymers feature high electromagnetic coupling, suggesting that efficient operation is possible. Furthermore they are relatively fast (bandwidths of 10 Hz up to tens of kilohertz). Dielectric elastomers have the further advantage of achieving large strains, which can exceed 100 %. A technical challenge encountered with dielectric elastomers and ferroelectric polymers is that they require high voltages, whereas only low battery voltages are available in most autonomous underwater vehicles.

The need for high voltages to drive dielectric elastomers and ferroelectric polymers can be resolved by employing compact DC-DC converters (e.g. EMCO High Voltage [21]). These would likely be placed in the after-body, where substantial space is available. High voltages would then be transmitted down the shaft to the propeller. At present the cost of the DC-DC converters and the continuous drain on power are too high to be practical for application in EMATT.

Conducting Polymer Actuators: Conducting polymer actuators that employ polypyrrole as the active material feature work densities in the range of 85 to 100 J/m^3 [22,23], an order of magnitude larger than the minimum required. They also operate at low voltages and feature a catch state in which virtually no current is drawn. These actuators are electrochemical in nature, requiring two electrodes separated by an electrolyte. Application of a voltage between the electrodes, one or both of which are polymer, leads to changes in polymer dimension as charges are added or removed from the polymer and ions are inserted or removed in order to maintain charge balance.

Three principal challenges are encountered in using polypyrrole actuation. The first is that the strains are typically ~ 2 % [2], requiring mechanical amplification, and the second is that lamination of thin films or fibers will be required in order to produce acceptable actuation rates. Finally, although polypyrrole actuators can be run in salt water [24], the lack of control over the solute concentration and content will likely lead to unreliable performance and a method of encapsulation is required.

Mechanical Amplification: Polypyrrole actuators are capable of producing 2 % strains at 5 MPa. Since the force needed to deflect the trailing edge flap, divided by the cross-sectional area of the blade and multiplied by the relative moment arms (3.5 N/(50 mm×6 mm)×7 mm/3mm=28 kPa) is much less than the stress that the actuator is capable of generating, no amplification of the force is required. In fact the force per cross-sectional area can be reduced by two order of magnitude if needed to magnify the displacement.

If the strain multiplied by the length of the actuator is roughly equal to the required displacement required at the tendon attachment point on the trailing edge then little or no amplification of the strain is required, simplifying design and fabrication. The strain required to directly drive the actuator without mechanical amplification is the displacement needed divided by the actuator length. The actuator length is constrained by the 15 mm length of the leading edge (Figure 2). The displacement is determined by the attachment point to the trailing edge and the angular deflection. Assuming that the attachment point is 3 mm above the joint and that a total angular deflection of at most 22^o is needed, then the 'ideal' strain is 15 %. Clearly there is a need to amplify the 2 % strains that are typically observed in polypyrrole actuators.

One possibility is to employ a recently reported method for obtaining 12 % strain in polypyrrole [25]. Although this approach is promising, the relatively large creep observed at reduced stresses and the lack of multi-cycle response data make it risky at present. Two methods of amplification are instead proposed and demonstrated on scaled prototypes.

Actuation Rate: In changing camber, a 1 to 10 s response time is sufficiently short for blade optimization during long periods of steady cruising. The actuator material thickness cannot exceed tens of micrometers if the actuator is to respond within ~ 10 s, due to mass transport limitations, as discussed by P. Madden in this issue [3,26]. In cases where high forces are required and width of the actuator is restricted, layering or folding of thin actuator sheets may be necessary so that the force and speed specifications can both be met. Such lamination will be needed in order to meet the force and displacement specifications set out for the EMATT vehicle, as will be discussed, and represents a design and fabrication challenge.

Electrical Connections. The polypyrrole actuators employed in this study behave electrically as enormous capacitors and feature a capacitance per unit volume of 10^8 F/m^3. As a result the resistance must also be limited in order to minimize RC charging times [3,28]. Thus multiple electrical contacts with the polymer and minimal separation between electrodes are essential [28].

IV. Design Approach & Results

Two mechanical amplification methods are used. One is a bending trilayer [27-29] which operates like a bimetallic strip. Two thin sheets of polypyrrole are laminated together, separated by a thin layer of gel electrolyte, forming a trilayer structure. Application of a potential difference between them causes one sheet to expand and the other to contract, producing bending. In the second approach linear contraction of the polypyrrole is amplified by two sequential cantilevers to generate the required displacement.

The initial objective is to demonstrate the operation of a variable camber foil in air and in pure water. Geometry and flow conditions are chosen to be consistent with those of the MIT water tunnel. A deformable portion at the trailing edge of the wing is designed to act as an aileron, generating torques consistent with flow rates of up to 1 m/s and a 44^o bending angle.

A. *Bending Trilayer*

The foil geometry, shown in Figure 3, is approximately NACA 0014 (no camber, thickness is 14 % of chord). The span is 240 mm, the average chord length is 70 mm and the maximum thickness is 34 mm. Camber is varied by deforming a rectangular polypyrrole actuated section that is

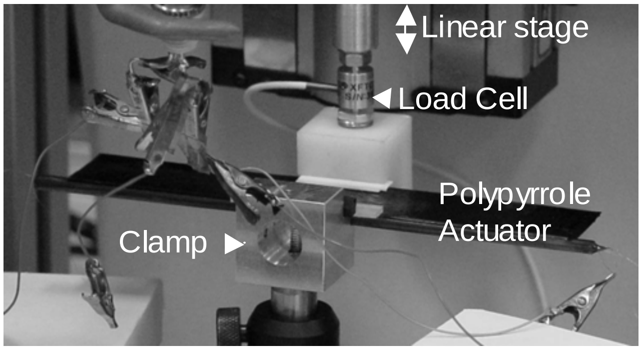

Fig. 6. Force measurement apparatus. The bending actuator (black) is held horizontally and clamped on each of its long sides to prevent motion. Electrical activation produces a vertical force, as measured by a load cell.

150 mm long, 30 mm wide and ~ 0.12 mm thick. The actuating section is inserted into a groove in the foil and fixed in place using polyurethane adhesive. In this actuation mechanism, the application of potential between two polymer layers separated by a gel electrolyte causes one to swell and the other to contract, leading to bending. Equations of a bimetallic strip were adapted for a three layer structure to determine the layer thicknesses necessary to produce the desired ±30 degree deflection [30]. The forces required to maintain the deflection given a flow speed of ~ 1m/s (for water tunnel testing) were also considered in designing the structure. Calculations based on the flow speed and geometry predict that a force of 0.15 N needs to be maintained on the trailing edge. The actuator is designed to achieve this force.

1) Synthesis & Fabrication

The active portion of the foil consists of five main components as depicted in Figure 4: 2 layers of polypyrrole (PPy), a paper separator (Kodak EK1546027) which prevents electrical shorting, gold wire providing electrical contact (75 µm diameter), laminated muscovite mica shims which prevent spanwise bending, and gel electrolyte. Construction of the trilayer begins with electro-deposition of 30 µm thick films of hexafluorophosphate-doped PPy onto a glassy carbon crucible following a previously described procedure [31]. Once removed from the glassy carbon, two pieces of PPy are cut to the desired geometry (150 mm x 30 mm). Two 150 mm long, 5 mm wide muscovite mica shims (~350 µm thick) are laminated together to serve as a mechanical restraint to span-wise bending. These form the trailing edge of the active portion of the foil.

Synthesis of the gel electrolyte is based on a procedure described by Noda and Watanabe [32]. The gel is prepared from a mixture of 10 g (40 Mol·%) of 1-Butyl-3-methylimidazolium tetrafluoroborate, 8.41 g (58.4 mol·%) of 2-Hydroxyethyl methacrylate, 0.175 g (0.8 mol·%) of Ethylene glycol dimethacrylate and 0.8 g (0.145 mol·%) of Azobisisobutyronitrile. All ingredients are stirred together. The starting substances are obtained from Sigma-Aldrich.com.

During fabrication, one sheet of PPy is placed on a Teflon surface. Gold wire is placed along one side of the sheet's major axis to provide electrical contact. Next, a sheet of lens paper is laid down. Laminated muscovite mica is placed along the major axis. The electrolyte gel is then spread evenly over the paper and a second gold wire in put down. The second PPy sheet is placed over the sample. A sheet of Teflon is temporarily placed over the entire trilayer and the layers are clamped between two metal plates. The trilayer is placed in an oven and baked at 80 °C for 12 hours. Encapsulation is achieved using a 3.5 µm thick polyethylene terephthalate film (www.goodfellow.com) which is folded over the trilayer and sealed with flexible polyurethane (Kalex® D-50, www.elementis-specialties.com). A syringe and needle are used to remove excess air as the urethane seal is compressed.

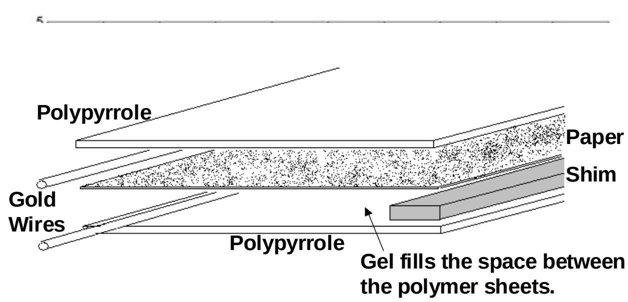

Fig. 4. Layered structure of the active section (not to scale). 30 µm thick PPy sheets (top and bottom), are separated by a paper spacer. A 350 µm thick mica shim (bottom right) provides spanwise rigidity at the trailing edge and 75 µm diameter gold wires (left), form electrical contacts. The space between the PPy sheets is filled with gel electrolyte. The total thickness is approximately 120 µm, except at the shim. An encapsulating layer of very thin mylar film covers the entire structure (not shown).

Fig. 5. Spanwise view of foil (looking from the blade tip), showing the neutral (left) and deflected (right) states during actuation in air.

± 3 V steps. The asymmetries in the
d 300 s are associated highly oxidized

2) Results

Step potentials of ± 2.5 V are applied to the polymer actuator in air to actively and reversibly change camber. Figure 5 depicts the foil with the span almost perpendicular to the camera and the chord oriented vertically and demonstrating a 35° orientation change of the active member (black). The deflection shown is achieved in 4 s.

Force testing is performed by fixing both ends of the active member and applying ±3 V potential steps. A ± 2 N range load cell (XFTC-101, www.GSSensors.com) was used to measure forces, in combination with a Vishay 2311 signal conditioning amplifier, www.vishay.com). A photograph of the force measuring apparatus is shown in Figure 6. The recorded potential, current and force are plotted in Figure 7. Generated forces exceed the minimum 0.15 N with the actuator held in the undeflected position. It takes 25 s or more for most of the force change to occur, significantly slower than the 4 s observed in the unloaded films. This slower response results at least in part from the fact that after 4 s the bilayer has not achieved full deflection, whereas the actuation over 25 s is nearly complete, as demonstrated by the saturation in force.

Stiffness is tested by recording force as a function of trailing edge deflection. Figure 8 shows the force in response to ±1 mm deflections. The deflections are induced via a stepper motor and linear stage (Zeta drive, www.compumotor.com), to which the load cell is attached.

The trailing edge deflects by less than 1 mm under a normal force of > 0.15 N. This is a very important result, as it indicates that the actuator is capable of withstanding the design forces without significant deflection.

Experimentation in water is at an early stage. Actuation is observed in shallow water. The encapsulation is breached when submerged to depths of greater than ~ 1 m. This leakage has prevented water tunnel testing.

3) Scaling

Tests to date have been performed on a larger foil to enable characterization in the MIT water tunnel. In order to apply this technology to EMATT forces need to be scaled up from 0.15 N to 3.5 N, while angular deflections need to be maintained. Geometrical relationships are used to determine the thicknesses of the polymer layers that will enable the same angular displacements to be achieved in the EMATT propeller as are achieved in the foil geometry shown in Figure 3.

Two bending structures achieve the same angular deflection if their ratios of segment length to radius of curvature are the identical. Therefore the ratio of the curvatures must equal the ratio of segment lengths. The trailing edge segment of the structure in Figures 3 and 5 is 30 mm long, whereas 10 mm is desired in the final EMATT design. The radius of curvature on the EMATT trailing edge must then be 1/3rd that of the flap demonstrated here. In both bilayer and trilayer actuators, in which displacement is achieved by contracting one layer of a laminated structure relative to the other, the ratio of the total thickness of the structure to the radius of curvature is given by a constant multiplied by the relative difference in strain [30,33], providing in the trilayer case that the relative thicknesses of the central layer and the outer layers remains constant. These relationships also assume the same relative change in oxidation state is induced in both cases. Thus in order to achieve the same angular displacement in the EMATT propeller as has been achieved in the polymer actuated foil, the trilayer used in the EMATT propeller must be 1/3rd as thick, or approximately 40 micrometers total. The two polypyrrole layers, which are 30 µm thick in the experiments presented here, must now be 10 µm thick, and the gel layer that was previously 60 µm thick is now reduced to 20 µm.

The ratio of forces F_2/F_1 can is determined by taking the ratio of forces for [30,33]:

$$\frac{F_2}{F_1} = \frac{W_2 \cdot t_2^{\,2}}{W_1 \cdot t_1^{\,2}} \cdot \frac{L_1}{L_2} \qquad (1)$$

where W represents trilayer width (spanwise), t represents thickness, and L is the length (chordwise). Once again Equation 1 is only valid if the two trilayers have the same ratios of polymer to gel thicknesses, and consist of the same materials. The ratio of forces is known (3.5 N / 0.15 N), as are the lengths (L_1=30 mm, L_2=10 mm) and thicknesses (from the geometrical arguments above, t_2/t_1=1/3). The width, W_1 is 150 mm, enabling W_2 to be evaluated. The resulting width, W_2 is 2.1 m. The actual width, W_2 is 50 mm at best, or 42

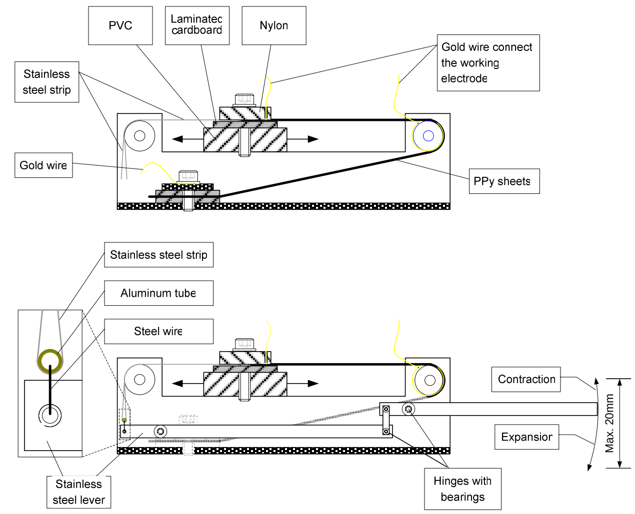

Fig. 10. Side view diagram of the linear actuator driven foil. The top diagram shows how polypyrrole sheets (black in fig. 9) are fixed to the base at one end. From the base, the strips cross diagonally up to a cylinder (blue in fig 9) that rolls on two bearings (at either end). The strips are then clamped to a moveable truck. Two thin stainless steel ribbons (50 µm thick, 5 mm wide) extend from the far side of the trucks, one on each side of the device, and are wound around another roller (left side in this figure, top cylinder in fig 9). The ribbons are each attached to a beam. As polypyrrole contracts, the left ends of the beams are pulled upwards, rotating them about their bearings. The far ends of the beams displace downwards, with 5 × greater displacement than the left ends, due to the placements of the bearings. The beams each pull a second cantilever, which again has a 5 × amplification factor, with the result that the right hand tip of the second cantilever deflects upwards by 25 × the initial displacement of the polymer. The cantilevers in fig. 8 move out of the page. Gold wires make electrical connections to the polypyrrole films.

operation is described in Figure 10. The geometry is designed to match that of the trilayer actuated configuration, with the 150 mm between cantilevers, and the 30 mm protruding length (bottom of Figure 9) matching the dimensions of the trilayer flap in Figure 3. Polypyrrole actuation is achieved by placing the entire apparatus into an organic solvent salt bath and applying potential between the polypyrrole films and a

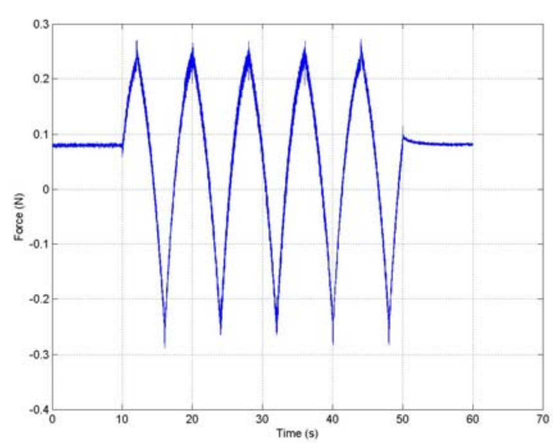

Fig 8: Stiffness of the variable camber trailing edge. A 1 mm amplitude triangular wave displacement is applied, generating the forces shown.

counter electrode. (In the final version, the electrolyte and counter electrode will be encapsulated within the foil structure.) Synthesis of the polymer films follows the procedure described above. A potentiostat is employed in order to set an applied voltage [34]. Load is varied by applying weights to the cantilevers (e.g. the wrench shown in Figure 9). The force exerted on the foil is calculated based on the applied mass and the buoyancy of the electrolyte. Displacements are recorded by video camera, and currents and voltages are recorded via an analog to digital converter.

Results

Figure 11 depicts the extent of deflection obtained by driving the mechanism using a voltage range of 3.5 V. A 33^o displacement occurred in 12 minutes under a load of 0.65 N. Stresses produced by the polypyrrole actuator are estimated to reach 7 MPa, and strains are just over 1 %, based on observed changes in position of the trailing edge. The work density achieved is 70 MJ/m^3. Initial currents observed upon the application of a step change in potential reach ~ 80 mA, and drop to < 30 mA within 15 minutes, as shown in Figure 12. Substantial parasitic current is observed, and is likely due to parasitic reactions at the surface of the steel frame (which can be eliminated by coating or encapsulation).

Rate: The 12 minute time to vary camber is much too slow to be practical. What limits the actuation rate and what are the opportunities for substantially reducing the actuation time? The initial current shown in Figure 12 suggests that series resistance of the cell is 40 ohms. Given the capacitance of conducting polymers, which can reach 10^8 F/m^3, and the available volume, the effective capacitance of the actuator film is 13 Farads. The RC time constant is calculated to be 500 seconds, or nearly 10 minutes, explaining the slow response. The rate will need to be improved by two orders of magnitude to make this approach feasible.

Scaling: In order to apply this technology to the EMATT, forces need to be scaled up from 0.65 N to 3.5 N while maintaining angular deflections. Furthermore the dimensions of the foil need to be reduced from 150 mm long in the active region and 70 mm wide, to 50 mm long and a total blade chord of 35 mm.

Desired displacements and strains can readily be scaled by reducing the size of the mechanism while maintaining mechanical advantage. The force can be increased by using more cross-sectional area of polymer. At present the cross-sectional area of polymer employed is 5×10^{-6} m^2. This will need to increase by a factor of 5.4 in order to produce 3.5 N, corresponding to a cross-sectional area of 27×10^{-6} m^2. The available width is reduced from 150 mm to 50 mm, and thus

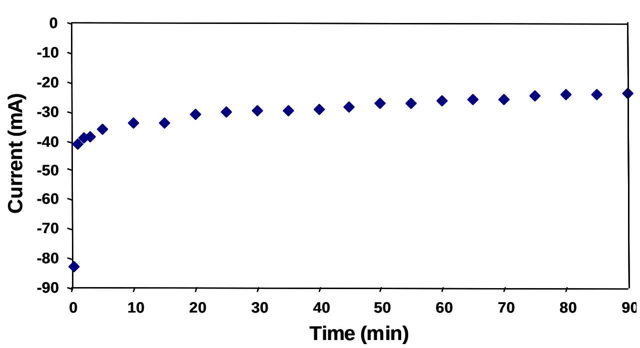

Fig 12: Current induced by the application of a step input of -3.5 V to the linear actuator. The current is accompanied by contraction of the polypyrrole and lifting of a 0.65 N weight.

the total polymer thickness must be 540 μm. This thickness corresponds to approximately 12 layers of polymer assuming actuator films are 43 μm thick. Thus the burden of mechanical amplification, in terms of needed layers of polypyrrole film, is not as severe as it is in the trilayer design.

Achieving the necessary improvement in rate is a real challenge in the linear actuator design. Scaling to the EMATT blade specifications will result in a need for more than double the volume of polymer, resulting in a corresponding increase in capacitance, and necessitating an overall reduction in cell resistance of more than 100 ×, to less than 0.4 Ω. Achieving this reduction in resistance can be achieved by interleaving the 12 layers with polymer counter electrodes, thereby minimizing the solution resistance. The current required to achieve fast actuation will also be correspondingly higher.

Cycle Life: Cycle life has not been addressed. More close to a million cycles are possible [35] using appropriate electrolytes similar to those used in this experiment.

VI. Discussion

Polypyrrole actuators are employed to generate variable camber foils. These foils achieve the appropriate range of deflection, but forces are as yet too small for the desired application. In order to increase force, parallel actuating films will be required, in which the placement of the counter electrodes must be carefully considered so that specified rates can be achieved. Encapsulation will also need to be improved. Given the increased forces in the final prototype tougher coatings can be used, increasing the chances of success.

References

[1] Y. Bar-Cohen Ed., *Smart Structure and Materials 2003*, *Electroactive Polymer Actuators and Devices, Proc. SPIE Vol. 5051,* 2003.

[2] J. D. Madden, N. Vandesteeg, P. A. Anquetil, P. G. Madden, A. Takshi, R. R. Pytel, S. R. Lafontaine, P. A. Wieringa and I. W. Hunter, "Artificial Muscle Technology: Physical Principles and Naval Prospects", *IEEE Journal of Oceanic Engineering* this issue.

[3] P. G. Madden, J. D. Madden, P. A. Anquetil, N. A. Vandesteeg and I. W. Hunter, "The relationship between conducting polymer actuator material properties and performance" *IEEE Journal of Oceanic Engineering* this issue.

[4] J. Hollerbach, I. Hunter & J. Ballantyne "A comparative analysis of actuator technologies for robotics", O. Khatib, J. Craig & Lozano-Perez Eds, *The Robotics Review* 2, MIT Press, Cambridge MA 1992, pp. 299-342.

[5] I. Hunter & S. Lafontaine, "A comparison of muscle with artificial actuators", *Technical Digest IEEE Solid State Sensors & Actuators Workshop*, 1992, pp. 178-185.

[6] The combustion of hexane produces ~ 40 MJ/kg and requires 19 Oxygen atoms. When the weight of oxygen is factored in, the energy per unit mass drops to ~ 4 MJ/kg. Lithium ion batteries have energy densities of ~ 0.6 MJ/kg (http://www.panasonic.com/industrial/battery/oem/chem/lithion/). Given that combustion engines are typically 1/3rd as efficient as high revving electric motors (30 % versus > 90 %), the relative advantage of combustion is reduced to a factor of 2, not including the mass and bulk of the oxygen storage vessel and of the transmission system.

[7] M.S. Triantafyllou, A.H. Techet, and F.S.Hover, "Review of experimental work in biomimetic foils", *IEEE Journal of Oceanic Engineering* this issue.

[8] G. S. Triantafyllou, M. S. Triantafyllou and M. A. Grosenbaugh in *Journal of Fluids and Structures,* Vol. 7, No. 2, pages 205-224; 1993.

[9] J.D. Madden, "Actuator Selection", *Proceeding of SPIE Smart Structures and Materials: Electroactive Polymer Actuators and Devices*, Y. Bar-Cohen ed. Bellingham, WA: SPIE Press, 2004, in press.

[10] Honda Motor Company, Online content available at: http://world.honda.com/ASIMO/P3/spec/, 2004.

[11] F.W. Riegels, *Aerofoil sections*. London: Butterworths, 1961.

[12] K. Brownlie, *Controllable pitch propellers*, London, Witherbys, 1998.

[13] Allen, B., W.S. Vorus, and T. Prestero 2000. Propulsion System Performance Enhancements on REMUS AUVs. *Proc. MTS/IEEE Oceans 2000*, 2000.

[14] Abbott, I.H., and A.E. von Doenhoff, Theory of wing sections. New York: Dover, 1959.

[15] Sippican, personal communications and web based specifications http://www.sippican.com 2003. BAE systems personal communication regarding power train.

[16] P. R. Bandyopadhyay, *A biomimetic propulsion for active noise control : experiments,* NUWC-NPT Technical Report 11,351, Naval Undersea Warfare Center, March 2002.

[17] D.Reynaerts, W. Van Moorleghem, H. Van Brussel, "Design and construction of a stepping shape memory actuator for driving a variable camber aircraft wing", *Proceedings of the 10th IEEE Conference on Advanced Robotics*, 2001.

[18] C.H. Beauchamp.; R.H Nadolink; S.C. Dickinson; L.M. Dean, "Shape memory alloy adjustable camber (SMAAC) control surfaces" *European Conference on Smart Structures and Materials*, 1992, p 189.

[19] For example the Futaba S3101 micro servo has dimensions of 28 mm × 12.7 mm × 30 mm, a mass of 17 grams and generates a torque of 25 mN·m at 4.8 V or 32 mN·m at 6 V. The volume is twice as large as the maximum available. The torque to volume ratio is 3000 N·m/m^3 and the torque to mass ratio is ~ 2 N·m/kg. Online content available at http://www.futaba-rc.com/servos/futm0029.html.

[20] Hollerbach, J.M., Lang, J., Vaaler, E., Garabieta, I., Sepe, R., Umans, S., and Hunter, I.W., `` The McGill/MIT Direct Drive Motor project," *Proc. IEEE Intl. Conf. Robotics and Automation,* May 2-7, 1993, Atlanta, pp. 2:611-617.

[21] EMCO High Voltage, Online content available at http://www.emcohighvoltage.com/ 2004.

[22] GM Spinks, DZ Zhou, L Liu, GG Wallace, "The amounts per cycle of polypyrrole electromechanical actuators", *Smart materials and structures*, 12 (3): 468-472, 2003.

[23] J. D. Madden, P. G. Madden, and I. W. Hunter, Conducting polymer actuators as engineering materials. In: *Proceeding of SPIE Smart Structures and Materials 2002: Electroactive Polymer Actuators and Devices*, ed. Yoseph Bar-Cohen. Bellingham, WA : SPIE Press, 2002.pp. pp. 176-190.

[24] A polypyrrole actuator was operated by Patrick Anquetil, MIT, using water collected at Revere Beach, Massachusetts for a period of 1 hour at a rate of approximately ~0.1 Hz and applied voltage amplitudes of 2 to 3 V versus a stainless steel counter electrode. Significant deposits formed on the polypyrrole, which could lead to degradation in response over longer time periods. Oxidation of the stainless steel also occurred, leading to strong discoloration of the electrolyte.

[25] L.Bay, K.West, P.Sommer-Larsen, S.Skaarup & M.Benslimane, "A conducting polymer artificial muscle with 12% linear strain", *Advanced Materials*, Vol. 15, p. 310-313, 2003.

[26] Madden, J. D., Madden, P. G., and Hunter, I. W. Characterization of polypyrrole actuators: modeling and performance. In: *Proceedings of SPIE 8th Annual Symposium on Smart Structures and Materials: Electroactive Polymer Actuators and Devices*, ed. Yoseph Bar-Cohen. Bellingham WA: SPIE, 2001.pp. 72-83.

[27] T.F. Otero, J. Rodriguez, E. Angulo, C. Santamaria, "Artificial muscles from bilayer structures", *Synthetic Metals*, 55-57, 3713-3717, 1993.

[28] Q. Pei, O. Inganas, "Electrochemical application of bending beam method", *Journal of Physical Chemistry*, 96(25), 10507-10514, 1992.

[29] Zhou DZ, Spinks GM, Wallace GG, Tiyapiboonchaiya C, MacFarlane DR, Forsyth M, Sun JZ "Solid state actuators based on polypyrrole and polymer-in-ionic liquid electrolytes", *Electrochimica Acta* 48 (14-16): 2355-2359, 2003.

[30] P.G. Madden, MIT Mechanical Engineering Ph.D. Thesis, Ch. 4, 2003.

[31] M. Yamaura, T. Hagiwara, and K. Iwata, "Enhancement of electrical conductivity of polypyrrole film by stretching: counter ion effect", *Synthetic Metals*, vol. 26, pp. 209-224, 1988.

[32] A. Noda, and M. Watanabe, *Electrochimica Acta*, vol. 45, pp. 1265-1270, 2000.

[33] J.D. Madden & C.J. Brenan, "Progress towards an automatic microfabricated polymer air-fluid sampling inlet", prepared for the Defense Advanced Research Project Agency, United States Department of Defence, National Technical Information Service, Order Number: AD-A332 030/6, November 1997. (available for download at www.ntis.gov).

[34] J. D. Madden, R. A. Cush, T. S Kanigan, and I.W. Hunter, "Fast contracting polypyrrole actuators", *Synthetic Metals*, vol. 113, pp. 185-193, May, 2000.

[35] Lu W, Fadeev AG, Qi BH, Smela E, Mattes BR, Ding J, Spinks GM, Mazurkiewicz J, Zhou DZ, Wallace GG, MacFarlane DR, Forsyth SA, Forsyth M, "Use of ionic liquids for pi-conjugated polymer electrochemical devices" *Science* 297 (5583): 983-987, 2002.

John D. Madden (M'95) was born in Ottawa, Canada in 1968. He received a B.Sc. in Physics from the University of British Columbia (UBC), Vancouver, Canada in 1991, an M.Eng. in Biomedical Engineering from McGill University, Montreal, in 1995 and a Ph.D. from the BioInstrumentation Lab at MIT in 2000. Dr. Madden left MIT for UBC in 2002 and is currently an Assistant Professor of Electrical & Computer Engineering. His research involves fundamental studies & applications of polymer and nanotube actuators and electronic devices.

Bryan Schmid was born in Buffalo, New York in 1981. He received his B. Sc. in mechanical engineering from the Massachusetts Institute of Technology, Cambridge, Massachusetts in 2003. Bryan is currently pursuing his M. Sc. degree at MIT.

He has performed research for Molecular Mechanisms, LLC. His current research interests include mechanical design and conducting polymer technologies as part of the BioInstrumentation Lab at MIT.

Mr. Schmid is the recipient of the Padmakar P. Lee Student Award and was a representative of the United States for the International Design Competition in 2002. He is also a member of Pi Tau Sigma, the mechanical engineering honor society.

Serge Lafontaine is a scientific consultant whose interest is the development of medical and bio-medical instrumentation. Serge spent two years as Post-Doctoral fellow at the BioInstrumentation Laboratory at MIT after completing his Ph.D. in the department of Biomedical Engineering at McGill University. Serge completed first a B.Sc. in Physics at the University of Montreal and still keeps an interest in physics and instrumentation in general. His main research interests include sensors and actuators including conducting polymers and shape memory alloys, data acquisition and control mainly applied to the development of new devices for the characterization of materials and systems, optics, electronics and software algorithms. Serge has developed a wide-field optical imaging system for the quantitative detection of fluorescence in high-throughput massively parallel drug discovery, genetic engineering and diagnostic system and a fully digital imaging and beam control system of an electron microscope. Serge has participated in the creation of several new businesses including Biotrove Inc. and LifeFX Technologies Inc..

Peter Madden was born in Ottawa, Canada in 1971. He received a B.A.Sc. in Engineering Physics from the University of British Columbia (UBC) in 1993, an M.Eng. in Biomedical Engineering from McGill University, Montreal, in 1996 and a Ph.D. in Mechanical Engineering from MIT in 2003. He is currently an Post-doctoral Associate in the Department of Organismic and Evolutionary Biology at

Harvard University. His current research is in the area of fish pectoral fin propulsion and maneuvering.

Ian W. Hunter was born in New Zealand in 1953. He received the B.Sc., M.Sc., D.C.P. and Ph.D. degrees in science at the University of Auckland, in Auckland, New Zealand in 1974, 1975, 1976, and 1980, respectively. He was affiliated with McGill University in Montreal, Canada from 1980 until 1994 when he joined the faculty of MIT in Cambridge, Massachusetts where he presently is the Hatsopoulos Professor of Mechanical Engineering, a Professor of Biological Engineering, and head of the BioInstrumentation Lab. His current research interests are micro-instrumentation, micro-fabrication, micro-robotics, micro surgical robotics, artificial muscle fibers, laser imaging systems, and instrumentation physics.